Available online at www.sciencedirect.com
ScienceDirect
Automatica 43 (2007) 876–884
automatica
www.elsevier.com/locate/automatica

Brief paper

Control of dynamic keyhole welding process☆

Y.M. Zhang*, Y.C. Liu

Center for Manufacturing and Department of Electrical and Computer Engineering, University of Kentucky, Lexington, KY 40506, USA

Received 20 November 2005; received in revised form 19 May 2006; accepted 6 November 2006
Available online 8 March 2007

Abstract

Weld joint penetration control is a basic research topic in the welding research community. The authors propose using an innovative plasma arc welding process referred to as the quasi-keyhole process to achieve less application-dependent weld joint penetration sensing and control. To control the quasi-keyhole process, the peak current and keyhole sustaining current are selected as the control variables to maintain the keyhole establishment and sustaining periods at desired values. The dynamic quasi-keyhole process is approximated by a linear model with interval parameters. A control algorithm has been developed for the multivariable interval quasi-keyhole process based on a predictive control algorithm for interval SISO models. Experiments have been conducted to test the effectiveness of the control system developed.

Keywords: Manufacturing; Intervals; Robust control; Predictive control; Interval model; Welding; Penetration; Keyhole; GTAW; PAW

1. Introduction

Gas tungsten arc welding (GTAW) has been the primary process for precision joining of metals and for critical applications such as the root pass where the weld joint penetration must be assured. The majority of research in arc welding process sensing and control has been devoted to GTAW especially to the sensing and control of the weld joint penetration in GTAW. The issue here is to assure the production of a desired full penetration as shown in Fig. 1(b) without occurrence of either partial penetration (Fig. 1(a)) or over-penetration (Fig. 1(c)), or maintain the back-side bead width w_b within a certain specified range. In the current practice, a highly skilled and experienced human welder is needed to observe the weld pool and adjust the welding parameters accordingly if the variations or changes in manufacturing conditions may exist. Unfortunately, human welders do not typically perform consistently because high concentration must be maintained during the labor-intensive operation in a difficult and arduous working environment. In addition, for new applications, the operators need significant practice in order to develop specific skills. Hence, automated sensing and control of joint penetration is an issue the welding research community must address and for which to find good solutions.

One of the major criteria for a good solution is that the sensor used can be attached to and move with the welding torch to be qualified as a front-side sensor which measures the welding process from the front-side of the workpiece. Because the objective is to maintain the back-side bead width within a certain range using a front-side sensor, the invisibility of the back-side and the strong arc light radiation appear to be the major obscures and various methods have thus been proposed, including pool oscillation, ultrasound, infrared sensor, etc. The pioneering work in pool oscillation was conducted by Kotecki, Richardson, and Hardt (Kotecki, Cheever, & Howden, 1972; Renwick & Richardson, 1983; Zacksenhouse & Hardt, 1984). Ouden (Anedenroomer & den Ouden, 1998; Xiao & den Ouden, 1993) found an abrupt change in the oscillation frequency of the pool during the transition from partial to full penetration. Ultrasound based weld penetration sensors have been extensively investigated at the Idaho National Engineering Laboratories. At Georgia Institute of Technology, Ume (Graham & Ume, 1997; Hopko & Ume, 1999) leads the development of non-contact ultrasonic penetration sensors based on laser-phased array techniques. Because the temperature distribution in the weld zone

☆ This paper was not presented at any IFAC meeting. This paper was recommended for publication in revised form by Associate Editor Pedro Albertos under the direction of Editor Mituhiko Araki.

* Corresponding author. Tel.: +1 859 257 6262x223; fax: +1 859 323 1035.
E-mail address: ymzhang@engr.uky.edu (Y.M. Zhang).

0005-1098/$ - see front matter © 2007 Elsevier Ltd. All rights reserved.
doi:10.1016/j.automatica.2006.11.008

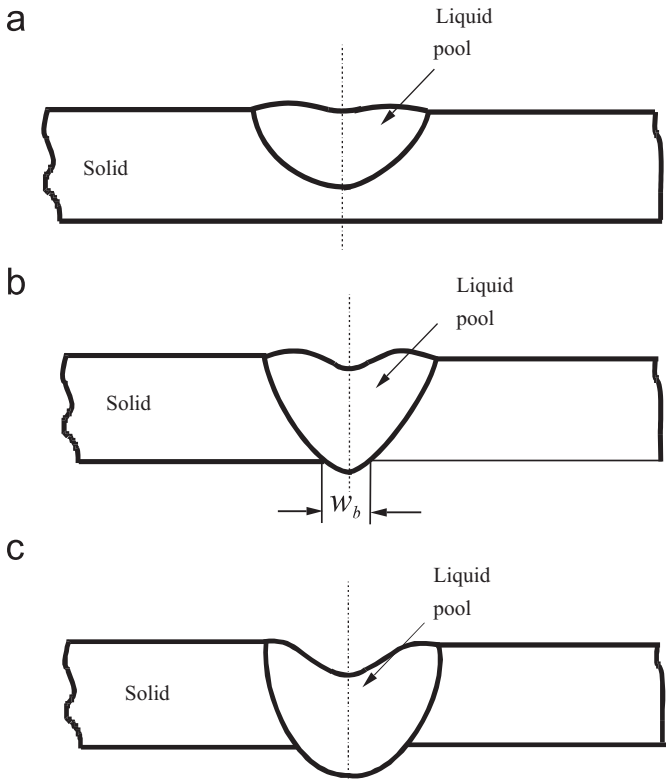

Fig. 1. Weld pool and penetration: (a) partial penetration; (b) full penetration; (c) over-penetration.

contains abundant information about the welding process, infrared sensing of welding processes has been explored by Chin at Auburn University (Banerjee et al., 1995; Chen & Chin, 1990; Nagarajan, Banerjee, Chen, & Chin, 1992; Wikle, Zee, & Chin, 1999). The penetration depth of the weld pool has been correlated with the infrared characteristics of the infrared image. At MIT, Hardt used an infrared camera to view the temperature field from the back-side (Song & Hardt, 1993). The penetration depth was estimated from the measured temperature distribution and then controlled (Song & Hardt, 1994).

Although existing methods can be effective for specific applications targeted and deserve further study, they are typically very application dependent and require sophisticated, application-oriented studies before being applied. To obtain technologies which can be more application independent and require much less application orientation studies before being applied, innovative methods are needed. To this end, the authors propose using an innovative keyhole plasma arc welding (PAW) process as a substitute for GTAW for more application-independent sensing and control of weld joint penetration.

2. Proposed method

In melt-in processes like GTAW, the heat is applied on the surface of the base metal and the base metal is melted by heat transferred from the surface. While their major advantage is that they are relatively easy for human welders to operate and control because of the relatively slow process, their low heat efficiency and large distortion are often concerns. High-energy beam welding processes including electron beam, laser, and PAW process can vaporize or displace part of the molten metal in the weld pool to form a hole penetrating completely through the base metal as referred to as keyhole (AWS, 1990). The presence of the keyhole allows the heat/energy be directly imposed on the base metal underneath the surface of the base metal to greatly improve the heat efficiency and reduce the distortion. The major disadvantage associated with the keyhole process appears to be more difficult to control than the relatively slow melt-in GTAW process, but the authors will show below how the keyhole process can actually be taken advantage of to ease the weld joint penetration sensing and control.

First, the authors propose to use PAW process to achieve keyhole because of its low cost. In name, PAW sounds quite different from GTAW; but PAW is actually a slight modification of GTAW by adding an orifice to restrict the arc in order to achieve a denser energy beam (AWS, 1990) and the equipment cost is just slightly higher than that of GTAW. When the tungsten electrode locates within the torch nozzle and the orifice, the arc is restricted and the highly constrained arc or plasma jet can displace the molten metal in the weld pool to form a keyhole completely through the base metal (AWS, 1990).

Second, the keyhole is associated with a fundamental change in the process. Before the keyhole is established, the gaseous cavity (front surface of the weld pool) produced by the arc pressure and the back-side surface of the workpiece are divided by the weld pool and solid metal. The ionized shield gas or plasma jet must bounce back from the workpiece (Zhang, Zhang, & Liu, 2001). After the keyhole is established, the gaseous passage from the front to the backside of the workpiece is formed. As a result, the plasma jet can pass from the front to the back and at least part of the plasma jet will not bounce back but exit from the backside of the workpiece as efflux plasma. This fundamental change associated with the keyhole establishment has led to the development of a few simple yet effective and application-independent sensors either by measuring the efflux plasma or the reflected plasma (Lu, Zhang, & Emmerson, 2004; Zhang & Zhang, 2001; Zhang et al., 2001).

Third, the welding current is applied at the peak level to provide peak level of heat input until the keyhole be established but is then switched to the base level after the keyhole establishment is confirmed or after the keyhole has been established for a specified short period. If the welding speed is faster or the plate is thicker, the peak current will be automatically applied for a longer time in order to establish the keyhole. Because the keyhole is only established very briefly and will close after the current is switched to the base level, this mode of operation is referred to as quasi-keyhole process. It is apparent that using the quasi-keyhole process, the control of the weld joint penetration to achieve the desired full penetration can be application-independent if (1) the peak level of the heat input is high enough so that the keyhole will be established in a reasonable period of time and (2) the base level of the heat input is low enough so that the keyhole will close in a reasonable period of time.

While a few sensors have been developed, the control of the quasi-keyhole process has been focused on the establishment

of the keyhole (Lu, Zhang, & Lin, 2003; Zhang & Walcott, 2006). To fully take advantage of the quasi-keyhole process, its full dynamics including the keyhole establishment and keyhole closure must also be controlled simultaneously. This paper thus addresses the control of the full dynamics of the quasi-keyhole process in order for the keyhole to be established and maintained in reasonable or desired periods. It is expected that the developed control method can be combined with different sensors to provide solutions to different applications.

3. Experimental system

The experimental set-up is shown in Fig. 2. The power supply is an inverter designed for GTAW and PAW. Its current ranges from 10 to 400 A and is controlled by an inner-loop controller. The controller adjusts the welding current through the analog output interface to the power supply. The torch, a regular commercial straight-polarity PAW torch rated at 200 A, is attached to a manipulator. The motion of the manipulator is computer controlled.

The keyhole sensor used in this study is referred to as the efflux plasma charge sensor (EPCS) (Zhang & Zhang, 2001). As discussed earlier, after the keyhole is established, the plasma jet must exit from the keyhole. The efflux plasma establishes an electrical potential between the workpiece and the detection plate, which is electrically isolated from the workpiece, due to the phenomena of plasma space charge (Li, Brookfield, & Steen, 1996). However, if the keyhole is not established, there will be no efflux plasma between the workpiece and the detection plate, and thus no electrical potential established. Hence it is possible to measure the electrical potential, or the voltage between the workpiece and the detection plate, to determine if the keyhole is present.

The experiments conducted in this study will be bead-on-plate welding on 3.6 mm thick stainless steel (type 304). The

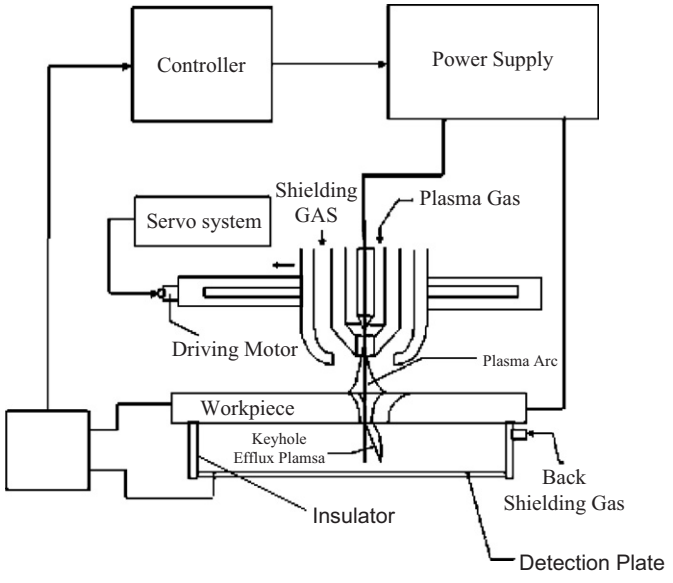

Fig. 2. Experimental set-up.

Table 1
Constant welding parameters

Diameter of electrode	3.2 mm
Orifice diameter	2.4 mm (0.078 in)
Flow rate of plasma gas	2.3 L/min (5 ft^3/h)
Flow rate of shielding gas	16.1 L/min (35 ft^3/h)
Flow rate of backing gas	18.4 L/min (40 ft^3/h)

diameter of the plasma orifice was 2.4 mm. Table 1 gives the values of those parameters being constant during experiments. Other welding parameters which are subject to change will be given later for the specific experiment or specific type of experiments conducted.

4. Controlled process

The controlled quasi-keyhole process proposed in this paper is illustrated in Fig. 3. At $t = t_1$, the peak current (I_p) is applied; the control system keeps detecting the signal from the keyhole sensor; before the keyhole is established, the output of the keyhole sensor is zero; at $t = t_2$, the keyhole is established and the keyhole sensor signal jumps to a few volts. In quasi-keyhole process, the current can be switched from I_p to the base current (I_b) at $t = t_2$ so that the keyhole is closed immediately. However, a rapid closure of the keyhole may not be preferred and a direct switch from the peak to base current should be avoided. In the controlled quasi-keyhole process proposed, the keyhole may remain open for a specified period. To this end, the current is first reduced from the peak level I_p to a lower level I_k (referred to as the keyhole sustaining current) in a pre-specified time period ($t_4 - t_2$) at a relatively slow slope and then reduced to the base level I_b at a relatively rapid (pre-specified) slope. In this way, if the keyhole does not close before t_4, it must close after t_4. (In Fig. 3, for illustration purpose the keyhole closure time t_3 is plotted before t_4 and the case where the keyhole closure time t_3 occurs after t_4 is not shown.) After I_b is applied for a period so that $t_6 - t_3 = T_b$ where T_b is a per-specified period, the current is switched to the peak level I_p again to begin a new cycle.

It is apparent that a complete quasi-keyhole cycle has three periods: (1) keyhole establishment period T_p during which the peak current is applied to establish the keyhole; (2) keyhole sustaining period T_k during which the keyhole remains open; (3) cooling period T_b during which the current is reduced to and then remains at the base level I_b. The dynamic behavior of the quasi-keyhole process is primarily determined by T_p and T_k and it is apparent that it is possible and convenient to control them by adjusting I_p and I_k. Hence, the controlled process has two outputs (T_p and T_k) and two inputs (I_p and I_k) and the feedback of the outputs can be measured from the keyhole sensor signal as can be seen in Fig. 3. The objective of the control system is to adjust I_p and I_k to maintain T_p and T_k at the desired levels. To this end, effort is needed to model the controlled process first.

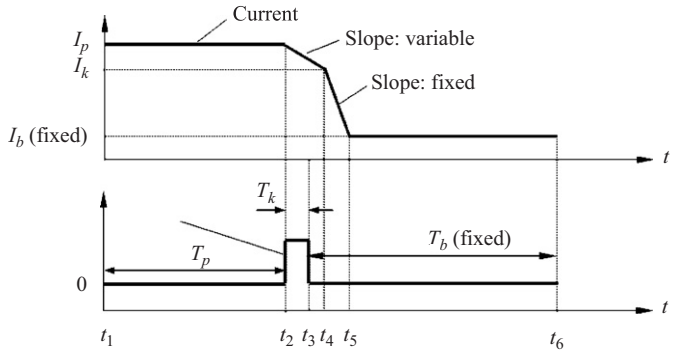

Fig. 3. Controlled quasi-keyhole process.

5. Modeling

For the arc welding process, the parameters in its dynamic model change with the welding conditions. However, the welding conditions do not change the structure of its dynamic model since its governing equations (a set of partial differential equations) do not change. Hence, the arc welding process can be described using a model with interval parameters, which is referred to as an interval model (Dehleh, Tesi, & Vicino, 1993). For the quasi-keyhole process, the major welding conditions which may affect its dynamics include the welding speed and the arc length.

To model the quasi-keyhole process, two sets of experiments have been conducted under two sets of experimental conditions, specified by welding speed and arc length as given in Table 2. Experimental data are then analyzed using the least-squares algorithm and F-test to identify the model structure and parameters (Liu, 2004). For data set 1, the following model structure is obtained:

$$\begin{cases} T_p(k) = a_0 + a_2 I_p(k-1) + a_3 I_p(k-2) \\ \qquad\quad + a_4 I_p(k-2) T_p(k-1), \\ T_k(k) = b_0 + b_1 I_k(k-1) + b_2 T_p(k). \end{cases} \tag{1}$$

For data set 2, the obtained model structure is

$$\begin{cases} T_p(k) = a_0 + a_1 T_p(k-1) + a_2 I_p(k-1) \\ \qquad\quad + a_4 I_p(k-2) T_p(k-1), \\ T_k(k) = b_0 + b_1 I_k(k-1) + b_3 I_p(k-1) T_p(k), \end{cases} \tag{2}$$

where a_j's and b_j's are parameters which may have different values in (1) and (2).

It can be seen that both model structures include non-linear terms. However, it is found

$$\begin{cases} T_p(k) = c_p + a_{p1} I_p(k-1) + a_{p2} I_p(k-2) \\ \qquad\quad + a_{p3} I_p(k-3) + b_{p1} T_p(k-1), \\ T_k(k) = c_k + a_{k1} I_k(k-1) + d_1 T_p(k) \end{cases} \tag{3}$$

are reasonable approximations for model structures (1) and (2). In fact, in comparison with (1), the standard deviation of the model residual for data set 1 is only increased 1% when using (3) for T_p (Liu, 2004). In comparison with (2), the standard deviations for data set 2 are only increased 3.3% and 3.7%, respectively, for T_p and T_k using their linear approximations in (3) (Liu, 2004).

Table 2
Bounds of parameters of identified model

Experimental condition		a_{p1}	a_{p2}	a_{p3}	b_{p1}	a_{k1}	d_1
Speed (mm/s)	Arc length (mm)						
2.24	5.2	−1.7984	0.3573	0.0540	0.5425	1.5481	0.0405
3.63	8.2	−4.3277	0.5376	0.3750	0.2374	0.6239	0.0281

Using model structure (3), two sets of model parameters have been fit from the two sets of experimental data acquired from two typical experimental conditions. It is known that the experimental conditions as specified by welding speed and arc length affect the model parameters. In the practical manufacturing environment, these conditions do change and generate significant process uncertainty (parameter range) so that the improvement using the non-linear model becomes insignificant and that the linear model structure (3) can be used as a reasonable approximation for the dynamics of the quasi-keyhole process. Further, the parameters in the model structure used should not be treated as fixed values. Instead, they can be treated as parameter ranges or intervals.

To obtain the intervals of the model parameters, experiments can be done at different sets of experimental conditions. The two sets of experimental conditions listed in Table 2 can be considered as two extreme conditions. In this study, 2.0 mm/s is selected as the minimal speed desired. A shorter arc length can produce a deeper penetration but a too short arc length may cause the undesired double-arc, i.e., part of the arc be established between the orifice and the workpiece; and 5 mm is set as the minimal arc length in this study. Increasing the welding speed and arc length improve the productivity and help prevent the undesired double-arc, but at the expense of reducing the penetration capability. Hence, 3.5 mm/s and 8 mm are selected as the maximal speed and arc length. In experiment 1, the condition which produces approximately the deepest penetration is used. The condition used in experiment 2 is the condition which approximately produces the shallowest penetration. Hence, the two experiments can be considered as two extreme conditions and the two sets of the identified parameters shown in Table 2 can be used to estimate the intervals of the model parameters.

In conclusion, the dynamics of the quasi-keyhole process under this study can be described using an interval model:

$$\begin{cases} T_p(k) = c_p + [-4.3277, -1.7984] I_p(k-1) \\ \qquad\quad + [0.3573, 0.5376] I_p(k-2) \\ \qquad\quad + [0.0540, 0.3750] I_p(k-3) \\ \qquad\quad + [0.2374, 0.5425] T_p(k-1), \\ T_k(k) = c_k + [0.6239, 1.5481] I_k(k-1) \\ \qquad\quad + [0.0281, 0.0405] T_p(k). \end{cases} \tag{4}$$

Parameters c_p and c_k are determined by the operating point and do not provide insight into the process dynamics. They will not be used in the proposed control algorithm and are thus not listed in the table.

6. Interval model control system design

The predictive control which has found successful applications in many areas is selected for the control for the quasi-keyhole process. However, predictive controllers are traditionally designed primarily based on the nominal model without explicitly using the uncertainty of the controlled process (Clarke, Mohtadi, & Tuffs, 1987; Zhang, Kovacevic, & Li,1996). Campo and Morari (1987) and Allwright and Papavasiliou (1992) have developed predictive control algorithms for models with interval parameters. However, their efforts were toward the computational aspects and no performance results have been either given or proven. In a paper by Nicolao, Magni, and Scattolini (1996), a robust predictive control for uncertain impulse response functions with one uncertain parameter has been developed.

Min–max predictive control has been an active research area in recent years (Alamo, de la Pena, Limon, & Camacho, 2005; Lee & Cooley, 2000; Lu & Arkun, 2000; Ramirez, Arahal, & Camacho, 2004). The interval model predictive control problem is similar to a type of min–max predictive model control which addresses a family of plants (Lee & Cooley, 2000). In this type of min–max predictive model control, a cost function is formed using errors between the trajectory and the predictions of the future outputs/states. Because the predictions are not only the functions of the future control sequence but also functions of the model (in the family) or its parameters, they are uncertain and vary with the model or their parameters. All min–max predictive model control algorithms are solved as a min–max problem $\min_u \max_{\theta\in\Theta} J(\theta, u)$ where Θ presents a family of plants, u is the vector of the future control sequence, and $J(\theta, u)$ is the cost function. Algorithms have been developed to assure the stability for the resultant min–max predictive control systems. However, as recognized by Ramirez et al. (2004), the implementation of min–max model predictive control suffers a large computational burden due to the numerical optimization problem that has to be solved at every sampling time. Efforts have been made to develop computational manageable algorithms. In the work by Ramirez et al. (2004), a neural network (NN) has been developed to approximate the solution of the min–max problem.

Zhang and Kovacevic (1997) proposed a predictive control algorithm for a class of SISO interval plants described using a finite impulse response (FIR) model. This algorithm and its implementation are relatively straightforward and it is now slightly modified for the control of the weakly coupled quasi-keyhole process which is modeled as

$$\begin{cases} T_p(k) = c_p + a_{p1} I_p(k-1) + a_{p2} I_p(k-2) \\ \qquad\quad + a_{p3} I_p(k-3) + b_{p1} T_p(k-1), \\ T_k(k) = c_k + a_{k1} I_k(k-1) + d_1 T_p(k) \end{cases} \tag{3a,b}$$

with the parameters as intervals as given in (4) in which the peak current duration $T_p(k)$ in (3b) is the only coupling term between the two subsystems. This type of weakly coupled system can be controlled by determining I_p from (3a) and then determining I_k from (3b) as two SISO systems.

To determine I_p from (3a) using the interval model algorithm proposed by Zhang and Kovacevic (1997), the ARMA model in (3a) needs to be converted into a FIR model. For convenience of derivation, let us denote $c_p = c_1$, $a_{11} = a_{p1}$, $a_{12} = a_{p2}$, $a_{13} = a_{p3}$, $b_{11} = b_{p1}$, $y_1(k) = T_p(k)$, $u_1(k) = I_p(k)$ and re-write (3a) as

$$y_1(k) = c_1 + \sum_{i=1}^{3} a_{1i} u_1(k-i) + b_{11} y_1(k-1). \tag{5}$$

Then

$$\Delta y_1(k) = \sum_{i=1}^{3} a_{1i} \Delta u_1(k-i) + b_{11} \Delta y_1(k-1), \tag{6}$$

where

$$\begin{cases} \Delta y_1(k) \triangleq y_1(k) - y_1(k-1), \\ \Delta u_1(k-i) \triangleq u_1(k-i) - u_1(k-i-1). \end{cases} \tag{7}$$

Because the system is stable, (6) can be approximated with a sufficient order n by

$$\Delta y_1(k) = \sum_{i=1}^{n} h_1(i) \Delta u_1(k-i), \tag{8}$$

where

$$\begin{cases} h_1(1) = a_{11}, \\ h_1(2) = a_{11} b_{11} + a_{12}, \\ h_1(j) = (a_{11} b_{11}^2 + a_{12} b_{11} + a_{13}) b_{11}^{j-3} \quad (j \geqslant 3). \end{cases} \tag{9}$$

Hence,

$$\begin{cases} y_1(k+1) = y_1(k) + \sum_{i=1}^{n} h_1(i) \Delta u_1(k-i+1), \\ \vdots \\ y_1(k+n) = y_1(k) + \sum_{i=1}^{n} h_1(i) \sum_{j=1}^{n} \Delta u_1(k-i+j). \end{cases} \tag{10}$$

Denote the n-step-ahead prediction using $u_1(k+1) = u_1(k+2) = \cdots = u_1(k+n) = u_1(k)$ (i.e., $\Delta u_1(k+1) = \Delta u_1(k+2) = \cdots = \Delta u_1(k+n-1) = 0$) as $y_1(k+n)|_{\Delta u_1(k)}$ where $*|_{\Delta u_1(k)}$ denotes the prediction made with $\Delta u_1(k) \neq 0$ as the last non-zero control change (i.e., all the future changes of the control $\Delta u_1(k+i) = 0$ $(\forall i > 0)$). Then,

$$\begin{aligned} y_1(k+n)|_{\Delta u_1(k)} &= y_1(k) + \sum_{i=1}^{n} h_1(i) \sum_{j=1}^{i} \Delta u_1(k-i+j) \\ &= y_1(k) + \sum_{i=1}^{n} h_1(i) \sum_{j=1}^{i-1} \Delta u_1(k-i+j) \\ &\quad + s_1 \Delta u_1(k), \end{aligned} \tag{11}$$

where $s_1 = \sum_{i=1}^{n} h_1(i)$ is the static gain of the subsystem. The control law proposed by Zhang and Kovacevic (1997) to control the interval model is

$$\max(y_1(k+n)|_{\Delta u_1(k)}) = y_{1s}, \tag{12}$$

where y_{1s} is the set-point for $y_1 = T_p$. (Zhang & Kovacevic, 1997 proved that this control law can guarantee the output converge to the set-point for any model whose parameters are bounded by intervals used in the control algorithm.) Hence,

$$\Delta u_1(k) = \frac{y_{1s} - \max(y_1(k+n)|_{\Delta u_1(k-1)})}{\tilde{s}_1}, \tag{13}$$

where

$$\tilde{s}_1 = \begin{cases} \max(s_1), & \Delta u_1 > 0 \\ \min(s_1), & \Delta u_1 < 0 \end{cases} \quad \text{and}$$

$$y_1(k+n)|_{\Delta u_1(k-1)} = y_1(k) + \sum_{i=1}^{n} h_1(i) \sum_{j=1}^{i-1} \Delta u_1(k-i+j).$$

When (13) is implemented, $\max(y_1(k+n)|_{\Delta u_1(k)})$ is computed for all uncertain parameters as specified by the intervals. As a result, (1) the predicted steady-state output is bounded by the set-point; (2) the control algorithm makes the predicted steady-state output to approach the set-point as aggressively as the model uncertainty (as specified by the parameters intervals) permits.

For the T_k subsystem, it is already in the FIR form and no conversion as for the T_p subsystem is needed. In addition, the order of the FIR model for this subsystem is 1. Hence, the control law is

$$\max(y_2(k+1)|_{\Delta u_2(k)}) = y_{2s}, \tag{14}$$

where $y_2(k) = T_k(k)$, $u_2(k) = I_k(k)$, $\Delta u_2(k) = u_2(k) - u_2(k-1)$ and y_{2s} is the set-point for $y_2 = T_k$.

Denote $a_{21} = a_{k1}$, $c_2 = c_k$. Eq. (3b) can be written as

$$y_2(k) = c_2 + a_{21} u_2(k-1) + d_1 y_1(k). \tag{15}$$

It can be shown that

$$y_2(k+1)|_{\Delta u_2(k)} = y_2(k) + a_{21}\Delta u_2(k) + d_1 h_1(1)\Delta u_1(k) + d_1 \sum_{i=2}^{n} h_1(i)\Delta u_1(k-i+1). \tag{16}$$

Here $\Delta u_1(k)$ has been determined by (13). Hence,

$$\Delta u_2(k) = \frac{y_{2s} - y_2(k) - \max(d_1 h_1(1)\Delta u_1(k) + d_1 \sum_{i=2}^{n} h_1(i)\Delta u_1(k-i+1))}{\tilde{a}_{21}}, \tag{17}$$

where

$$\tilde{a}_{21} = \begin{cases} \max(a_{21}), & \Delta u_2 > 0, \\ \min(a_{21}), & \Delta u_2 < 0. \end{cases}$$

The control algorithm for the quasi-keyhole process is thus given by (13) and (17).

7. Control experiments

The developed control algorithm has been used to conduct closed-loop control experiments under different conditions. The material used in experiments was stainless steel (type 304). The thickness of the plate was 3.6 mm and the dimensions of the workpiece were 250 mm × 50 mm. T_b, $t_4 - t_2$, and the slope in $[t_4, t_5]$ were fixed at 420, 20 ms, and 1.5 A/ms, respectively. The period of each weld cycle $T_p + T_k + T_b$ is variable since both T_p and T_k vary. Pure argon was used as the shielding gas and the orifice gas. The travel speed is 2 mm/s if not specified otherwise.

7.1. Nominally constant welding condition

Before the closed-loop control experiments are conducted, an open-loop experiment has been done with the constant inputs $I_p = 125$ A and $I_k = 105$ A. The corresponding output is plotted in Fig. 4. As can be seen, despite the constant input peak current and keyhole sustaining current, the resultant output keyhole establishing period fluctuates in addition to a shift with the time. This suggests that the process is subject to an inherent disturbance. Analysis shows that this disturbance is not caused by any external sources. Instead, it is a type of nature of the underlying process. In fact, as shown in a previous study (Ma, 2001), when the keyhole is being established, the process is in an unstable state. It is believed that during this unstable period, the geometry of the partial (non-penetrated) keyhole experiences a strong fluctuation as determined by the balance between the surface tension, the plasma pressure, and the hydrostatic pressure before the keyhole is finally established. The establishment of the keyhole is thus subject to certain stochastic vibration or fluctuation. This inherent vibration or fluctuation places a difficulty for the control of the keyhole arc welding process. For T_k, it is observed that T_k fluctuates between 35 and 55 ms, indicating the keyhole sustaining procedure is not a stable process either, and introducing an inherent difficulty affecting control capability for T_k. However, the fluctuations in the keyhole establishment period and keyhole sustaining period do not affect weld quality in a significant way as long as the amplitudes are relatively small.

Fig. 5 shows a closed-loop control experiment under the nominally constant welding condition. In the first 20 weld cycles, the peak current was pre-programmed to fluctuate. During this period, the process model parameters are estimated under the nominal welding conditions in order to check if the pre-determined intervals are sufficient. After 20th weld cycle, the control action is applied. Because the inherent stochastic fluctuation is not controllable, the result in Fig. 5(a) actually shows a quite acceptable performance and the degree of fluctuation is similar as that in Fig. 4 since the amplitudes of the fluctuations in the keyhole establishment period and keyhole sustaining period are both comparable with those produced

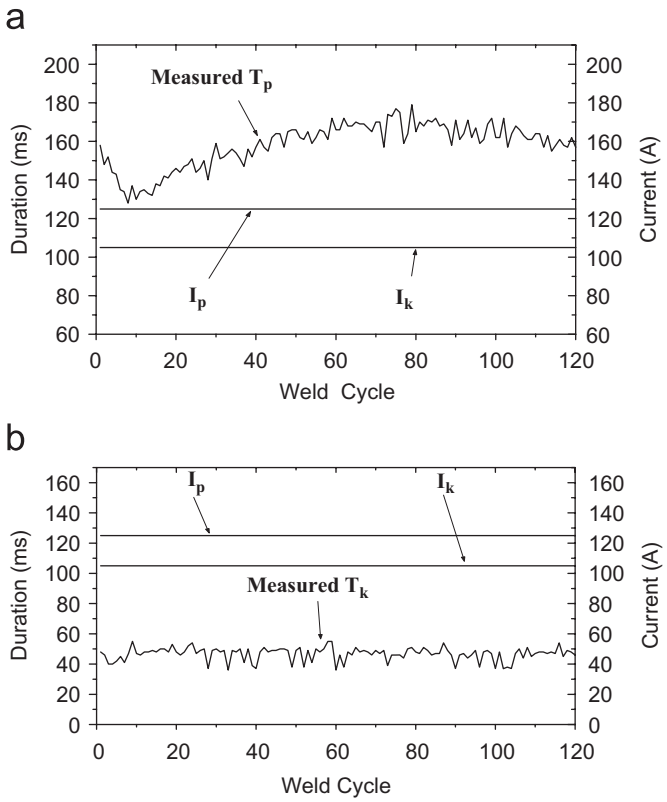

Fig. 4. System output T_p and T_k under constant input. (a) T_p, (b) T_k.

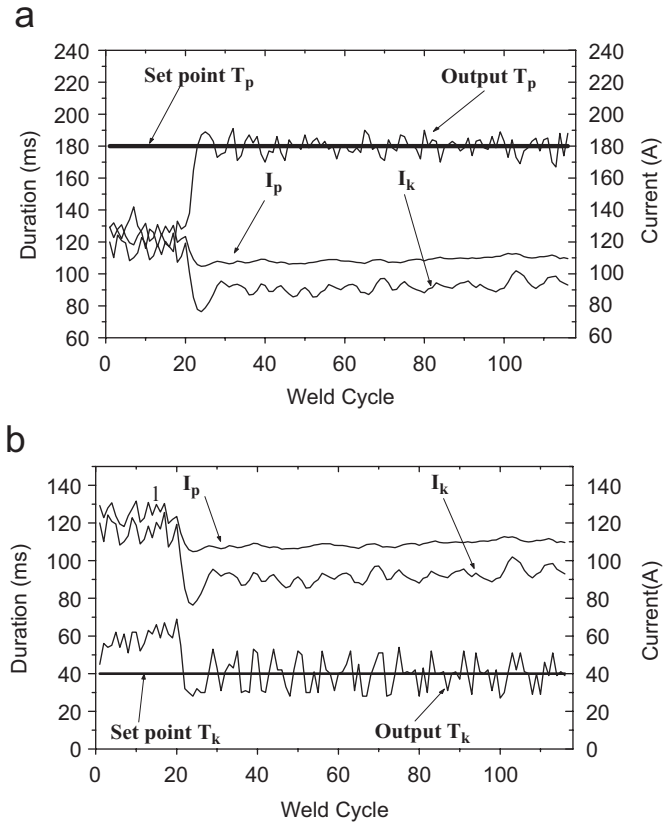

Fig. 5. Closed-loop control for constant set-point under normal condition. (a) T_p, (b) T_k.

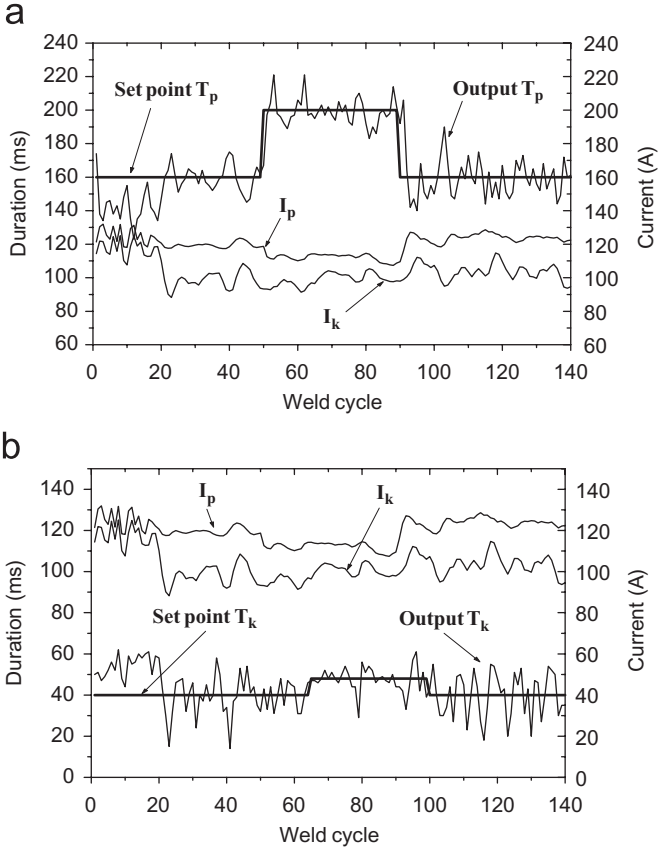

Fig. 6. Step set-point tracking. (a) T_p, (b) T_k.

using constant parameters. This indicates that the possible influence of the inherent stochastic fluctuation or disturbance on the closed-loop control system has been successfully suppressed.

7.2. Varied set-point

Varied set-point experiment is designed to verify the response speed of the interval-based predictive control system. The step set-point change is applied for T_p from 160 to 210 ms at the 50th weld cycle and then back to 160 ms at 90th weld cycle. The resultant output T_p and control variable I_p are plotted in Fig. 6. The set-point is also changed for T_k from 40 to 48 ms at 65th weld cycle and then back to 40 ms at 100th weld cycle. As can be seen, the output T_p can track the set-point change with an acceptable speed and accuracy. The tracking of T_k is still acceptable even small swing exists due to relatively unstable keyhole sustaining process.

7.3. Varying travel speed

The travel speed and the welding current are the two most important welding parameters determining the heat input into the workpiece. In this experiment, the travel speed changes from 2.1 to 2.4 mm/s at the 50th cycle, then back to 2.1 mm/s at the 90th cycle.

The output and control action after the speed increase at 50th cycle can be seen in Fig. 7. It is known that an increase in the

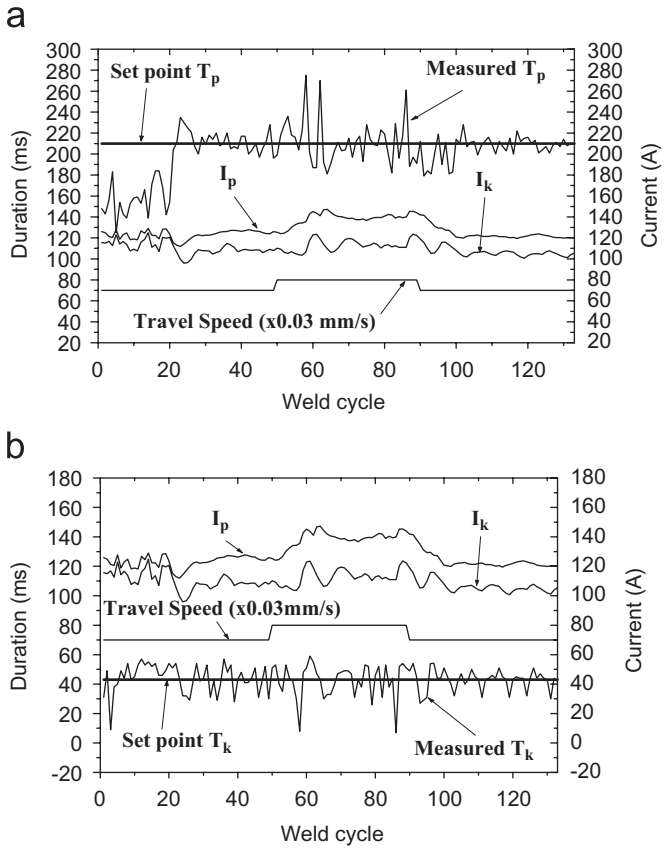

Fig. 7. Closed-loop control experiment under varying travel speed. (a) T_p, (b) T_k.

travel speed will cause a longer time for a given peak current to establish the keyhole. Hence, in order to maintain the output, i.e., the peak current period at the desired set-point, the peak current should increase. As can be seen in Fig. 7, after the speed is increased at 50th cycle, the peak current keeps increasing. As a result, the influence of the travel speed increase on the output is compensated. As it can be seen in Fig. 7, impacts of speed changes caused some fluctuations in the output T_p when the speed suddenly increases or decreases. However, there are no large fluctuations in T_k output. This is probably due to that the speed insignificantly affects T_k. The output T_p only briefly fluctuated around the set-point. The controller recognizes the error generated and adjusts the control variable. As a result, after a brief period of fluctuations, the T_p again returns back to set-point.

8. Conclusions

Dynamic keyhole behaviors as specified using the keyhole establishment time and keyhole sustaining time need to be controlled in order to optimize the operation of the quasi-keyhole process for better application independence. Inherent variations in the manufacturing conditions in a production environment require the control algorithm address the corresponding uncertainties in the model parameters. The interval model provides a convenient method to mathematically model these uncertainties as parameter intervals. The predictive control algorithm originally proposed for a class of SISO systems is used to develop a relatively less complicated control algorithm for the weakly coupled interval model of the quasi-keyhole process. Experiments verified that the dynamic quasi-keyhole process is controllable using the developed control system despite various variations in the manufacturing conditions and welding parameters.

Acknowledgments

This research is funded by the National Science Foundation under Grant DMI-0114982 and the University of Kentucky Center for Manufacturing.

References

Alamo, T., de la Pena, D. M., Limon, D., & Camacho, E. F. (2005). Constrained min–max predictive control: Modifications of the objective function leading to polynomial complexity. *IEEE Transactions on Automatic Control*, *50*(5), 710–714.

Allwright, J. C., & Papavasiliou, G. C. (1992). On-linear programming and robust model-predictive control using impulse-responses. *Systems & Control Letters*, *18*, 159–164.

Anedenroomer, A. J. R., & den Ouden, G. (1998). Weld pool oscillation as a tool for penetration sensing during pulsed GTA welding. *Welding Journal*, *77*(5), 181s–187s.

AWS (1990). *Welding handbook. Vol. 2: Welding processes* (8th ed.).

Banerjee, P. et al. (1995). Infrared sensing for on-line weld shape monitoring and control. *ASME Journal of Engineering for Industry*, *117*, 323–330.

Campo, P. J., & Morari, M. (1987). Robust model predictive control. In *Proceedings of 1987 American control conference* (pp. 1021–1026). Minneapolis, MN.

Chen, W., & Chin, B. A. (1990). Monitoring joint penetration using infrared sensing techniques. *Welding Journal*, *69*(4), 181s–185s.

Clarke, D. W., Mohtadi, C., & Tuffs, P. S. (1987). Generalized predictive control. *Automatica*, *23*, 137–160.

Dehleh, M., Tesi, A., & Vicino, A. (1993). An overview of extreme properties for robust control of interval plants. *Automatica*, *29*, 707–721.

Graham, G. M., & Ume, I. C. (1997). Automated system for laser ultrasonic sensing of weld penetration. *Mechatronics*, *7*(8), 711–721.

Hopko, S. N., & Ume, I. C. (1999). Laser generated ultrasound by material ablation using fiber optic delivery. *Ultrasonics*, *37*(1), 1–7.

Kotecki, D. J., Cheever, D. L., & Howden, D. G. (1972). Mechanism of ripple formation during weld solidification. *Welding Journal*, *51*(8), 386s–391s.

Lee, J. H., & Cooley, B. L. (2000). Min–max predictive control techniques for a linear state-space system with a bounded set of input matrices. *Automatica*, *36*, 463–473.

Li, L., Brookfield, D. J., & Steen, W. M. (1996). Plasma charge sensor for in-process, noncontact monitoring of the laser welding process. *Measurement Science and Technology*, *7*(7), 615–626.

Liu, Y. C. (2004). *Control of dynamic keyhole welding process*. Ph.D. Dissertation, Department of Electrical and Computer Engineering, University of Kentucky, September.

Lu, W., Zhang, Y. M., & Emmerson, J. E. (2004). Sensing of weld pool surface using non-transferred plasma charge sensor. *Measurement Science and Technology*, *15*(5), 991–999.

Lu, W., Zhang, Y. M., & Lin, W.-Y. (2003). Nonlinear interval model control of quasi-keyhole arc welding process. *Automatica*, *40*(5), 805–813.

Lu, Y. H., & Arkun, Y. (2000). Quasi-Min–Max MPC algorithms for LPV systems. *Automatica*, *36*, 527–540.

Ma, Y. (2001). *High speed image based stochastic analysis of dynamic plasma reflection behavior*. M.S. Thesis, Department of Electrical and Computer Engineering, University of Kentucky, May 2001.

Nagarajan, S., Banerjee, P., Chen, W. H., & Chin, B. A. (1992). Control of the welding process using infrared sensors. *IEEE Transactions on Robotics and Automation*, *8*(1), 86–93.

Nicolao, G. D. E., Magni, L., & Scattolini, R. (1996). Robust predictive control of systems with uncertain impulse response. *Automatica*, *32*, 1475–1479.

Ramirez, D. R., Arahal, M. R., & Camacho, E. F. (2004). Min–max predictive control of a heat exchanger using a neural network solver. *IEEE Transactions on Control Systems Technology*, *12*(5), 776–786.

Renwick, R. J., & Richardson, R. W. (1983). Experimental investigation of GTA weld pool oscillations. *Welding Journal*, *62*(2), 29s–35s.

Song, J.-B., & Hardt, D. E. (1993). Closed-loop control of weld pool depth using a thermally based depth estimator. *Welding Journal*, *72*(10), 471s–478s.

Song, J.-B., & Hardt, D. E. (1994). Dynamic modeling and adaptive control of the gas metal arc welding process. *ASME Journal of Dynamic Systems, Measurement, and Control*, *116*(3), 405–413.

Wikle, H. C., III, Zee, R. H., & Chin, B. A. (1999). Sensing system for weld process control. *Journal of Materials Processing Technology*, *89–90*, 254–259.

Xiao, Y. H., & den Ouden, G. (1993). Weld pool oscillation during GTA welding of mild steel. *Welding Journal*, *72*(8), 428s–434s.

Zacksenhouse, M., & Hardt, D. E. (1984). Weld pool impedance identification for size measurement and control. *ASME Journal of Dynamic Systems, Measurement, and Control*, *105*(3), 179–184.

Zhang, Y. M., & Kovacevic, R. (1997). Robust control of interval plants: A time domain approach. *IEE Proceedings—Control Theory and Applications*, *144*(4), 347–353.

Zhang, Y. M., Kovacevic, R., & Li, L. (1996). Adaptive control of full penetration GTA welding. *IEEE Transactions on Control Systems Technology*, *4*, 394–403.

Zhang, J., & Walcott, B.L. (2006). Adaptive interval model control of arc welding process. *IEEE Transactions on Control Systems Technology*, *14*(6), 1127–1134.

Zhang, S. B., & Zhang, Y. M. (2001). Efflux plasma charge-based sensing and control of joint penetration during keyhole plasma arc welding. *Welding Journal*, *80*(7), 157s–162s.

Zhang, Y. M., Zhang, S. B., & Liu, Y. C. (2001). Plasma cloud charge sensor for pulse keyhole process control. *Measurement Science and Technology*, *12*(8), 1365–1370.

YuMing Zhang has been with the University of Kentucky since 1991 where he is currently a Professor and the James R. Boyd Professor of Electrical Engineering. He was a faculty member from 1984 to 1991 in the State Key Laboratory for Advanced Welding Production Technology at the Harbin Institute of Technology, China where he received his Ph.D. degree in Mechanical Engineering/Welding Major, and M.S. and B.S. degrees in Electrical Engineering/Control Major. Dr. Zhang is a senior member of the IEEE and the SME, and a member of the AWS and the ASME. He received The Donald Julius Groen Prize from The Institution of Mechanical Engineers, United Kingdom; The A. F. Davis Silver Medal award from the American Welding Society; the Adams Memorial Membership Award from the American Welding Society; and the 15th IFAC Triennial World Congress Best Poster Paper Prize and Application Paper Honorable Mention from the International Federation of Automatic Control.

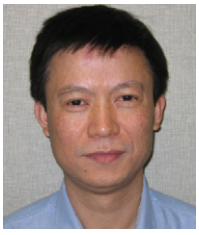

YuChi Liu is currently a Control Engineer at Magnatech Limited Partnership in East Granby, Connecticut, USA. He received his Ph.D. degree and an M.S. degree in Electrical Engineering from the University of Kentucky, Lexington, Kentucky, USA; an M.S. degree in Welding Major from Harbin Institute of Technology, Harbin, China; and his B.S. degree in Welding Major from Wuhan University of Hydraulic and Electrical Engineering, Wuhan, China. Dr. Liu is an AWS member. Dr. Liu received the 15th IFAC Triennial World Congress Best Poster Paper Prize and Application Paper Honorable Mention from the International Federation of Automatic Control.